Kinematic Control of Redundant Knuckle Booms

Björn Löfgren
Jan Wikander

ABSTRACT

The Swedish forestry industry competes on an international market; because raw material is more expensive than in other parts of the world, the chain from the stump to the industry needs to be very effective. One part in this chain is cutting and transporting trees from the forest to the landing area for further transportation with trucks to the paper or saw mill. When cutting and transporting trees, forestry machines equipped with booms are used to handle the trees. If boom handling time can be reduced thereby increasing productivity by 10 percent, the Swedish forestry industry can earn up to 250 million Swedish crowns (US$35 million) per year.

One way to decrease boom handling time is to introduce automatization. This paper describes how to solve the kinematic control of knuckle booms used on forestry machines when automatization is introduced. The objective was to develop a kinematic control strategy for maximum lifting capacity, which is suited for computer-controlled knuckle booms that are redundant. This strategy was analyzed with respect to time consumption when the manipulator tip moves along a predetermined path. The analysis was conducted on a knuckle boom used on a forwarder in a forestry application. The knuckle boom had one redundant degree of freedom. The analysis showed the necessary joint speed requirements and time consumption for certain motion cycles and also what happens when the joints reach their maximum velocity limits.

Keywords: *hydraulic manipulator, redundant, kinematic control, local optimization, knuckle boom, forest machine, forwarder, boom tip control, joystick control, simulations*

Introduction

A powerful and radical mechanization since the mid-1960s has made Swedish forestry almost 100 percent mechanized. This is one of the primary explanations as to why Swedish forestry could remain competitive in international markets.

Forestry machines of today are high technology units with advanced control engineering. Technology development has resulted in a radical increase in performance. For the operator this has meant an increased working volume and fewer natural stops in the ordinary work. At the same time, quality content in the operators' work has changed. It is no longer sufficient to control the machine and its functions. The operator also has responsibility for environmental concerns, planning, and follow-up of the work. Through the years, the working environment has improved resulting in less physical stress on the operator. But the increased working volume, in combination with many decisions that the operator has to make, has increased mental stress. The operator could be a bottleneck in new initiatives to increase productivity. By using more automated functions and letting the machine itself take care of repetitive work, it is possible for the operator to devote their time to decisions regarding tree selection, wood quality, and environmental concerns.

The control of the manipulator's movement takes most of the operators' working time on both forwarders and harvesters. There is a potential to simplify the control of the manipulator, partly to reduce the mental work load and produce a good effect on more important tasks, partly to increase the production. The risk for stress injuries can also be reduced. The control of the manipulator can be simplified through the introduction of a manipulator tip control and automated control of certain manipulator movements.

To control a forestry machine implies almost continuous precision work with the hands. High production requires intensive precision work. The repetitive work and the high intensity will cause statically tensed muscles and muscle fibers. In a harvester application, the operator uses the crane about 80 percent of the total work time. They cut one tree each 47 seconds and make 12 decisions/tree. On average they use 24 functions/ tree and cut about 1,000 trees/day. In a forwarder application, the operator uses the crane about 50 percent of the total work time. On average, they load and unload 1 tree each 30 seconds and handle about 400 trees/day.

Actions that increase blood running through the muscles are of crucial importance for minimizing the risk of stress injuries. The work to control the manipulator should, therefore, be as dynamic as possible, which requires many short pauses. Decreased demands on the precision of the joystick work will give less muscle tension and thereby reduce stress. Therefore, technical solutions that will give short pauses in the intensive joystick work are positive (Erikson and Thor 1999, Gellerstedt 1993).

Operators of forestry machines are exposed to great mental stress during their work. They have to receive and process a

The authors are, respectively, Lic. Tech., The Forest Research Institute of Sweden, Skogforsk, Uppsala, Sweden (bjorn.lofgren@skogforsk.se) and Professor, Mechatronics Lab, Department of Machine Design, Royal Institute of Technology, Sweden. This paper was received for publication in May 2007.

International Journal of Forest Engineering 20(1): 22-30.

large amount of information and make decisions under a great time pressure. At the same time, precision work with the hands means by itself a relatively large stress on brain activity (Gellerstedt 1993). A natural conclusion of this is that a simplified control of the manipulator can reduce the mental stress on the operator.

Forestry machines of today are controlled by two joysticks of different design. With the movement of one joystick in one direction, the operator is controlling a specific hydraulic actuator (cylinder) on the boom. This means that the operator has to combine different joystick movements to move the tip of the boom in the desired direction (**Fig. 1**).

The concept *boom tip control* means that the tip of the boom is controlled with only one joystick. Up/down on the joystick corresponds to up/down on the tip of the boom, out/in on the joystick corresponds to out/in on the tip of the boom, and left/right corresponds to left/right on the tip of the boom (**Fig. 2**).

With the extension, the linear degree of freedom (DOF) in the outer boom, in combination with the two rotational degrees of freedom, make it possible for the TCP (tool center point) to reach the next point on a desired path in a number of ways. In Löfgren (1989), computer analysis shows how the extension DOF affects the speed and the lifting force. The results show that the extension gives shorter time cycles and that one has better lifting force capacity close to the ground. This means that the extension should be included as much as possible in the kinematic control algorithm for the boom.

Joystick Control

As mentioned, the TCP is controlled with only one joystick. To have a good analogy between the joystick and the manipulator, the joystick functions are placed in the order shown in **Figure 3**. The swing function is placed in the left and right directions of the joystick.

Potential Advantages of Boom Tip Control

A simplified manipulator control will provide the following advantages compared to a conventional manipulator control:

- less physical strain on the operator,
- decreased learning time, and
- longer life time of the manipulator.

Operators of forestry machines are injured in the neck, shoulders, and back after some or several years of controlling the manipulator (Erikson and Thor 1999). More than half of all of the operators have had problems with the neck, shoulders, and back. These problems can be assigned to manipulator control.

It has been shown that operators unconsciously tense themselves before manipulator control work, with increased stress as a consequence (Erikson and Thor 1999). A simplified manipulator control will most likely influence the operators to control the manipulator in a more relaxed way.

Work with conventional control of knuckle booms is very complicated since one can reach every point within the knuckle boom's work space in many ways because the knuckle booms

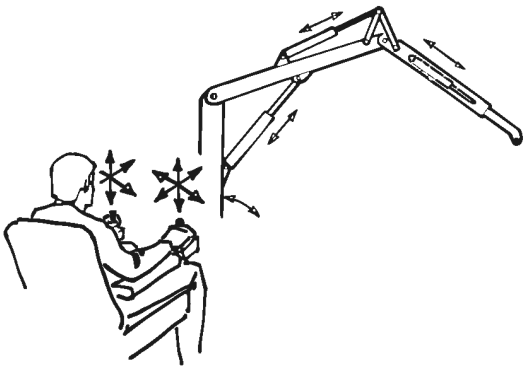

Figure 1. ~ *Conventional control.*

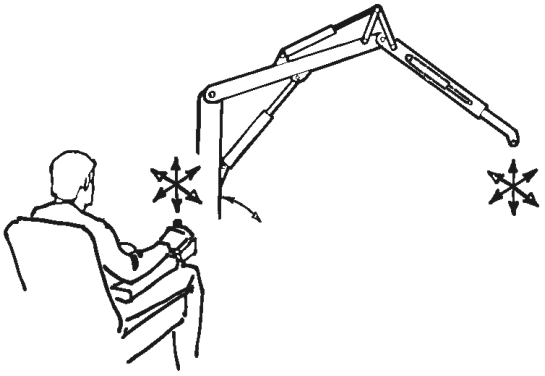

Figure 2. ~ *Boom tip control.*

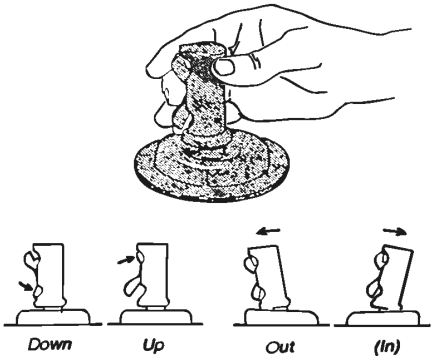

Figure 3. ~ *Joystick functions with boom tip control.*

are redundant. A simplified control will most likely make it easier to control the knuckle manipulator since the tip is controlled directly and since the redundancy is resolved automatically. Consequently, a simplified control will most likely mean that the learning time would decrease substantially (Suh and Hollerback 1987).

There is a big difference between a skilled operator and a non-skilled operator (Sciavicco and Siciliano 1987). A non-skilled operator will control the manipulator in a jerky way which will affect the lifetime of the manipulator. With a simplified control, it is possible to eliminate many of the jerky movements and, thereby, increase the lifetime of the manipulator.

Targeted Machines and Research Objectives

Most of the manipulators used in forestry are of a knuckle boom type. They are hydraulically powered and are controlled by hydraulic servo valves. The same types of hydraulic manipulators are also commonly used on trucks and in stationary applications. Knuckle booms are often constructed with extra DOF and are, therefore, redundant. A redundant manipulator, designed for positioning only, has more than three DOF. In this paper, a redundant manipulator with three revolute joints and one prismatic joint was studied.

Why is a redundant DOF introduced? The extra motor, sensor, etc., and the more complicated controller mean extra weight, complexity, and cost. Some objectives of the redundant DOF are:

- singularity avoidance,
- obstacle avoidance,
- robot dexterity,
- energy minimization,
- manipulator precision,
- lifting capacity, and
- velocity of operation.

This study was made possible by the introduction of computer control in a manually operated 4 DOF manipulator. The objective was to develop a kinematic control strategy to achieve maximum lifting capacity of a redundant knuckle boom. The strategy was to analyze based on time consumption when the manipulator tip moves along a predetermined path. The analysis was made on a knuckle boom used on a forwarder in a forestry application. The same type of manipulator geometry was used on other forestry machines and also on trucks.

State of the Art

A review of the research shows that there has been an increased interest in redundant manipulators since the beginning of the 1980s. Currently, in the academic world there is great interest in problems about kinematic redundancy.

Within the industry it was necessary to introduce one or more redundant DOF to solve complicated applications. The redundancy implies considerably more complicated control algorithms than those for non-redundant manipulators. Most of the methods used are based on local optimization and use the quite popular pseudo-inverse solution. The kinematic equation that describes the relation between manipulator end effector speed and corresponding joint speeds is defined as follows:

$$\dot{\underline{x}} = J\dot{\underline{\theta}} \qquad [1]$$

where:

$\dot{\underline{x}}$ = an $m \times 1$ velocity vector in Cartesian coordinates for the manipulator end effector,

$\dot{\underline{\theta}}$ = the $n \times 1$ joint velocity vector for the joints ($n > m$), and

J = the $[m \times n]$ Jacobian.

We solve the equation with respect to $\dot{\underline{\theta}}$:

$$\dot{\underline{\theta}} = J^{\#}\,\dot{\underline{x}} \qquad [2]$$

where:

$$J^{\#} = J^T (JJ^T)^{-1} \qquad [3]$$

$J^{\#}$ is the pseudo inverse of the Jacobian matrix according to the generalized Moore-Penrose inverse (Sciavicco and Siciliano 1987).

In Klein (1989), the problem with joint drift, when one uses only the pseudo inverse control, was analyzed for the case when a cyclic task was performed. Despite a well-developed theory in by Löfgren (1989), there was still a problem with making the control conservative (i.e., when repeating a work cycle several times, the joint configurations will not be repeatable and the manipulator can run into unfavorable configurations).

To overcome this drawback, a more general solution, by addition of a term, is given by:

$$\dot{\underline{\theta}} = J^{\#}\,\dot{\underline{x}} + (I - J^{\#}J)\dot{\underline{\phi}} \qquad [4]$$

where:

$\dot{\underline{\phi}}$ = an arbitrary joint velocity vector and

$(I - J^{\#}J)$ = the null-space projection matrix of J.

This corresponds to a self motion of the manipulator which has no effect on the velocity of the end effector. The attractiveness with this method is twofold. The first term, $J^{\#}\,\dot{\underline{x}}$, minimizes $\dot{\underline{\theta}}^T\,\dot{\underline{\theta}}$ (Sciavicco and Siciliano 1987), which presumably means that all of the joints will be prevented from moving too fast. The second term, $(I - J^{\#}J)\dot{\underline{\phi}}$, can improve the manipulator's configuration by assigning different optimization or performance criteria by means of a proper selection of $\dot{\underline{\phi}}$ (e.g., to achieve singularity avoidance) (Lögren et al. 1994).

Other secondary criteria are: obstacle avoidance (Klein and Kee 1989), joint torque optimization (Honegger and Codourey 1998, Noble 1975, Sciavicco and Siciliano 1987), joint velocity constraints (Beiner 1999, Cleary and Tesar 1990, Martin et al. 1989, Nedungadi and Kazerounian 1989), energy minimization (Beiner 1999, Chan and Dubey 1995, Klein 1985), manipulator precision (Klein 1985), speed of operation (Chan and Dubey 1995), joint limit avoidance (Chen et al. 1995), maximization of various end-effector dexterity measures (Klein and Kee 1989), multiple performance criteria (Chen et al. 1995, Erikson and Thor 1999, Nedungadi 1987), global optimization and global versus local optimization. Additional information about redundant manipulators can be found in Siciliano (1990).

Basic Equations

The studied manipulator (**Fig. 4**) is velocity-controlled by means of a 3-DOF joystick, operating in a cylindrical (r, θ, z) or Cartesian (x, y, z) coordinate system.

If we are working in the cylindrical coordinate system, the control of the θ_0 - motor is separated from the control of the other motors. If we are working in the Cartesian coordinate sys-

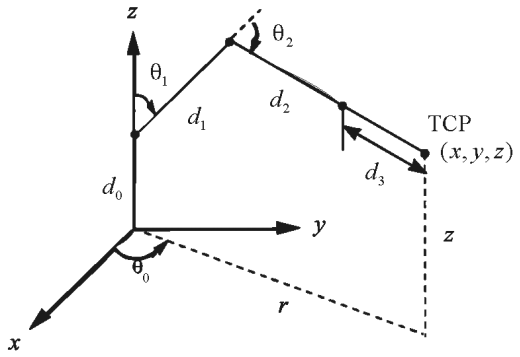

Figure 4. ~ *Manipulator geometry.*

tem, with commanded $\dot{x}$, $\dot{y}$, and $\dot{z}$, we find the commanded $\dot{\theta}_0$ by differentiating $\theta_0 = \arctan(y/x)$ and using:

$$r = \sqrt{x^2 + y^2}, \qquad [5]$$

$$\dot{\theta}_0 = (-s_0 \dot{x} + c_0 \dot{y}) / r, \qquad [6]$$

where:

$s_0 = \sin \theta_0$

$c_0 = \cos \theta_0$

The command $\dot{r}$ is found by differentiating $r = \sqrt{x^2 + y^2}$

$$\dot{r} = c_0 \dot{x} + s_0 \dot{y} \qquad [7]$$

We have now expressed the derivatives of x and y, and $\dot{x}$ and $\dot{y}$ as the derivatives $\dot{\theta}_0$ and $\dot{r}$, and can focus our study on the kinematic control in the r-z-plane, where the redundant DOF is used.

A vector $\underline{\theta}$ is defined:

$$\underline{\theta} = [\theta_1, \theta_2, d_3]^T \qquad [8]$$

The TCP coordinates r and z define the vector $\underline{x}$:

$$\underline{x} = [r, z]^T \qquad [9]$$

Figure 4 gives the following relations:

$$r = d_1 s_1 + (d_2 + d_3) s_{12} \qquad [10]$$

$$z = d_0 + d_1 c_1 + (d_2 + d_3) c_{12} \qquad [11]$$

where:

$s_{12} = \sin(\theta_1 + \theta_2)$,

$c_{12} = \cos(\theta_1 + \theta_2)$.

$$\dot{r} = d_1 c_1 \dot{\theta}_1 + (d_2 + d_3) c_{12} (\dot{\theta}_1 + \dot{\theta}_2) + s_{12} \dot{d}_3 \qquad [12]$$

$$\dot{z} = -d_1 s_1 \dot{\theta}_1 - (d_2 + d_3) s_{12} (\dot{\theta}_1 + \dot{\theta}_2) + c_{12} \dot{d}_3 \qquad [13]$$

or in matrix form:

$$\underline{\dot{x}} = J \underline{\dot{\theta}}, \qquad [14]$$

where the Jacobian J (2×3 – matrix) has elements $j_{11}, j_{12}, \ldots j_{23}$:

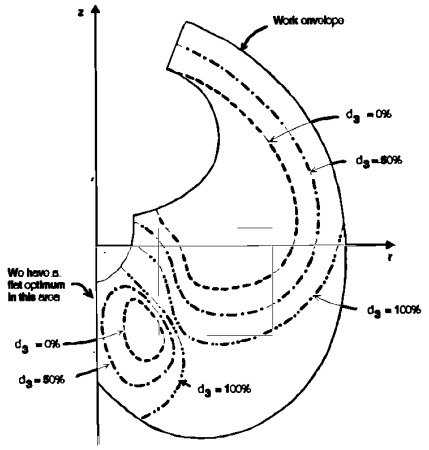

Figure 5. ~ *Selection of d_3 for maximum lifting capacity.*

$$J = \begin{bmatrix} d_1 c_1 + (d_2 + d_3) c_{12} & (d_2 + d_3) c_{12} & s_{12} \\ -d_1 s_1 - (d_2 + d_3) s_{12} & -(d_2 + d_3) s_{12} & c_{12} \end{bmatrix} \qquad [15]$$

Since the Jacobian J is not square, the matrix cannot be directly inverted. The problem can be solved by introducing a constraint.

A control strategy called maximum lifting capacity will be introduced in the following section.

Maximum Lifting Capacity

In some applications, the velocity is of major importance. It is not possible, however, to have maximum velocity as a constraint, since the operator will not use maximum velocity all of the time, but wants to utilize the highest possible velocity only when they find it necessary. In other applications, velocity is of minor importance, but for this application the static (low velocity) lifting capacity is essential. The kinematic control in this work was based on an optimization study of the lifting capacity (McGee et al. 1994), as a function of θ_1, θ_2, and d_3, based on the force or torque characteristics and the geometrical arrangements of the motors. From the studies, it is possible to analyze how the lifting capacity is dependent on the prismatic function d_3.

Figure 5 shows how d_3 should be chosen for maximum lifting capacity for a specific manipulator. Except for the lower left and upper middle part of the work area, the three curves (d_3 = 0%, 50%, and 100%) can be approximated by circles. In other cases, where the d_3-curves are more complicated, a look-up table for $d_3 = d_3(r, z)$ plus interpolation can be used.

In order to avoid unnecessarily large accelerations in d_3, some "smoothing" of the optimal $d_3(r, z)$ function may be introduced, especially in areas in the r-z plane where the optimum is flat, i.e., where the effect of d_3 on the lifting capacity is small. The proposed kinematic control of d_3 is shown in **Figure 6**.

From the analysis shown in **Figure 5**, the work space when $d_3 = d_{3\,\min}$ or when $d_3 = d_{3\,\max}$ could be compared to two circles with different radii's and origins (**Fig. 6**). The working area is

divided into two zones with equal width and the points A, B, C, and D are on the same straight line placed on the height z_C. The points A – D have the following coordinates:

A: (r_1, r_C)

B: (r_2, r_C)

C: $(r_i + \rho_{i\,\min}, z_C); i = 1,2$

D: $(r_i + \rho_{i\,\max}, z_C); i = 1,2$

Figure 6 gives:

$$\rho_i = \sqrt{(r - r_i)^2 + (z - z_C)^2} \qquad [16]$$

where r_i and r_C are the coordinates for the center point of the circles in the proposed kinematic control function.

The transition between $\rho_{i\,\min}$ and $\rho_{i\,\max}$ should be smooth. The choice of the coordinates for r_i and r_c can be done according to **Figures 5 and 6** and the geometrical data from a specific boom.

In the zone where d_3 is active, it should vary smoothly without large accelerations. We have chosen a function given in Equation [**17**] according to **Figure 7**. This function has $\frac{dd_3}{d\rho_i} = 0$ for $\rho_i = \rho_{i\,\min}$ and for $\rho = \rho_{i\,\max}$ thus avoiding jumps in d_3s velocity.

The smoothing function depicted in **Figure 7** is given by Equations [**17** through **19**].

$$d_3 = \frac{d_{3\,\max}}{2}\left[1 + \frac{3(\rho_i - p_i)}{2q} - \frac{(\rho_i - p_i)^3}{2q^3}\right] \qquad [17]$$

with

$$p_i = \frac{\rho_{i\,\max} + \rho_{i\,\min}}{2} \qquad [18]$$

$$q = \frac{\rho_{i\,\max} - \rho_{i\,\min}}{2} \qquad [19]$$

Differentiating Equation [**17**] gives:

$$\dot{d}_3 = f_i(r, \rho_i)\dot{r} + g_i(z, \rho_i)\dot{z} \qquad [20]$$

with

$$\begin{aligned} f_i(r,\rho_i) &= c(r - r_i)/\rho_i \qquad \rho_{i\,\min} \le \rho_i \le \rho_{i\,\max} \\ g_i(r,\rho_i) &= c(z - z_c)/\rho_i \quad for \quad \rho_{i\,\min} \le \rho_i \le \rho_{i\,\max} \\ f_i(r,\rho_i) &= g_i(z - \rho_i) = 0 \qquad \rho_i < \rho_{i\,\min}; \rho_i > \rho_{i\,\max} \end{aligned} \qquad [21]$$

where:

$$c_{ki} = \frac{3d_{\max}}{4q}\left[1 - \frac{(\rho_i - p_i)^2}{2q^2}\right] \qquad [22]$$

Independent of what characteristics we use for d_3 we can simplify our notations: $f_i(r, \rho_i) = f, g_i(z, \rho_i) = g$

Using $\dot{d}_3$ from Equation [**20**] in Equation [**16**] gives:

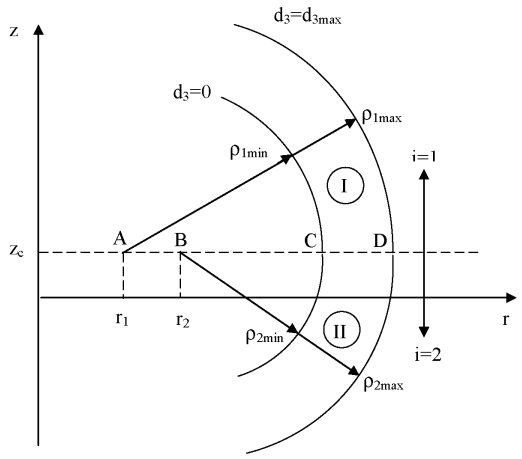

Figure 6. ~ *d_3 as a function of TCP position.*

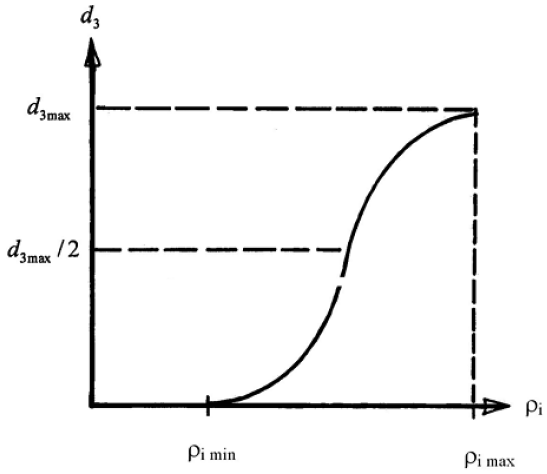

Figure 7. ~ *d_3 as a function of ρ_i*

$$\begin{bmatrix} \dot{r} \\ \dot{s} \end{bmatrix} = \begin{bmatrix} j_{11} & j_{12} & j_{13} \\ j_{21} & j_{22} & j_{23} \end{bmatrix} \cdot \begin{bmatrix} \dot{\theta}_1 \\ \dot{\theta}_2 \\ f\dot{r} + g\dot{z} \end{bmatrix} \qquad [23]$$

Rewriting Equation [**23**] gives:

$$\begin{bmatrix} j_{11} & j_{12} \\ j_{21} & j_{22} \end{bmatrix} \cdot \begin{bmatrix} \dot{\theta}_1 \\ \dot{\theta}_2 \end{bmatrix} = \begin{bmatrix} 1 - j_{13}f & -j_{13}g \\ -j_{23}f & 1 - j_{23}g \end{bmatrix} \cdot \begin{bmatrix} \dot{r} \\ \dot{z} \end{bmatrix} \qquad [24]$$

or

$$\begin{bmatrix} \dot{\theta}_1 \\ \dot{\theta}_2 \end{bmatrix} = \begin{bmatrix} j_{11} & j_{12} \\ j_{21} & j_{22} \end{bmatrix}^{-1} \cdot \begin{bmatrix} 1 - j_{13}f & -j_{13}g \\ -j_{23}f & 1 - j_{23}g \end{bmatrix} \cdot \begin{bmatrix} \dot{r} \\ \dot{z} \end{bmatrix} \qquad [25]$$

Equations [**20**], [**25**], and [**15**] give, after some calculations, the kinematic control law:

$$\dot{\underline{\theta}} = P\dot{\underline{x}} \qquad [26]$$

where the (3×2) P-matrix has the following elements:

$$\left.\begin{aligned} p_{11} &= D(s_{12} - f)/(d_1 s_2) \\ p_{12} &= D(c_{12} - g)/(d_1 s_2) \\ p_{21} &= D[d_1 f(c_2 f - s_1)/(d_2 + d_3) - s_{12}]/(d_1 s_2) \\ p_{22} &= D[d_1 g(c_2 g - c_1)/(d_2 + d_3) - c_{12}]/(d_1 s_2) \\ p_{31} &= f \\ p_{32} &= g \end{aligned}\right\} \quad [27]$$

where:

$$D = \frac{1}{d_1 (d_{23} - a c_2)} \quad [28]$$

Velocity Limitations

The motors have maximum velocities $\dot{\theta}_{1\,max}$, $\dot{\theta}_{2\,max}$, and $\dot{d}_{3\,max}$, respectively. If a motor, e.g., motor no. 1, receives a command signal $\dot{\theta}_{1c}$, with $|\dot{\theta}_{1c}| > \dot{\theta}_{1\,max}$, the velocity limitations will cause a position error. This problem is solved in the following way:

Introduce:

$$\left.\begin{aligned} \alpha_i &= |\dot{\theta}_{ic}| / \dot{\theta}_{i\,max};\ i = 1,2 \\ \alpha_3 &= |\dot{d}_{3c}| / \dot{d}_{3\,max} \end{aligned}\right\} \quad [29]$$

In a practical case, the geometrical arrangement of the θ_1 - and θ_2-motors (these revolute joints may be driven by hydraulic cylinders) may cause $\dot{\theta}_{1\,max}$ and $\dot{\theta}_{2\,max}$ to be functions of θ_1 and θ_2, respectively, and directions. In this case, joints speeds are set to equal in both directions. This is due to the fact that for each machine application, the hydraulic pressure and flow are different. Therefore, the joint speeds are set to suit one typical pressure and flow.

We find the largest α_i value, α_{max}:

$$\alpha_{max} = \max_{i=1,2,3}\{\alpha_i\} \quad [30]$$

If $\alpha_{max} \le 1$, there are no velocity limitations, and $\underline{\dot{\theta}}$, is as determined by Equation [**26**].

Assume that the joystick is working in the cylindrical coordinate system and that the θ_0- motor is separately controlled.

Assume $\alpha_1 = \alpha_{max} > 1$

Choose $\dot{\theta}_1 = \dot{\theta}_{1\,max}$ if $\dot{\theta}_1 > 0$ and $\dot{\theta}_1 = -\dot{\theta}_{1\,max}$ if $\dot{\theta}_1 < 0$. Since we have lost one DOF, i.e., the system is non-redundant, the calculation of $\dot{\theta}_2$ and $\dot{d}_3$ is straightforward. (r_c and z_c are commanded velocities.)

$$\begin{bmatrix} \dot{r}_c \\ \dot{z}_c \end{bmatrix} = J \begin{bmatrix} \pm\dot{\theta}_{1\,max} \\ \dot{\theta}_{2c} \\ \dot{d}_{3c} \end{bmatrix} \quad [31]$$

giving

$$\begin{bmatrix} \dot{\theta}_{2c} \\ \dot{d}_{3c} \end{bmatrix} = \frac{1}{D_1} \begin{bmatrix} j_{23} & -j_{13} \\ -j_{22} & j_{12} \end{bmatrix} \cdot \begin{bmatrix} \dot{r}_c \mp j_{11} \cdot \dot{\theta}_{1\,max} \\ \dot{z}_c \mp j_{21} \cdot \dot{\theta}_{1\,max} \end{bmatrix} \quad [32]$$

with

$$D_1 = j_{12} j_{23} - j_{13} j_{22} \quad [33]$$

To find out if the new values for $\dot{\theta}_{2c}$ and d_{3c} given by Equation [**32**] will exceed their maximum velocities, α_2 and α_3 must be calculated again giving α'_2, α'_3, and α'_{max}. If $\alpha'_{max} \le 1$, control law (Eq. [**32**]) is used. If $\alpha'_{max} > 1$, two motors, θ_1 and θ_2 or d_3 must be working at their maximum velocities and hence we now have only one DOF, and two DOFs are necessary to follow a commanded path in the r-z-plane.

Assume that $\alpha'_{max} = \alpha'_2$, i.e., $|\dot{\theta}_2| > \dot{\theta}_{2\,max}$. Choose $\dot{\theta}_2 > \dot{\theta}_{2\,max}$ if $\dot{\theta}_2 > 0$ or $\dot{\theta}_2 = -\dot{\theta}_{2\,max}$ if $\dot{\theta}_2 < 0$. The commanded velocity must be scaled by a factor $\beta < 1$ since we cannot follow the commanded path with two motors at their maximum speeds, due to the fact that we have lost two DOFs:

$$\beta \begin{bmatrix} \dot{r}_c \\ \dot{z}_c \end{bmatrix} = \begin{bmatrix} j_{11} & j_{12} & j_{13} \\ j_{21} & j_{22} & j_{23} \end{bmatrix} \begin{bmatrix} \pm\dot{\theta}_{1\,max} \\ \pm\dot{\theta}_{2\,max} \\ \dot{d}_3 \end{bmatrix} \quad [34]$$

Equation [**34**] has two unknowns, β and $\dot{d}_3$.

We find:

$$\beta = \frac{j_{23} k_1 - j_{13} k_2}{j_{23} \dot{r}_c - j_{13} \dot{z}_c} \quad [35]$$

and

$$\dot{d}_3 = \frac{\beta \dot{r}_c - k_1}{j_{13}} \quad [36]$$

where:

$$k_1 = \pm j_{11} \dot{\theta}_{1\,max} \pm j_{12} \dot{\theta}_{2\,max} \quad [37]$$

$$k_2 = \pm j_{21} \dot{\theta}_{1\,max} \pm j_{22} \dot{\theta}_{2\,max} \quad [38]$$

If instead $\alpha'_{max} = \alpha'_{3\,max}$ similar calculations will apply.

Similar calculations will apply also if we have speed limitations in θ_2 or d_3, i.e., $\alpha_2 = \alpha_{max}$ or $\alpha_3 = \alpha_{max}$.

Mechanical Limitations

If one of the θ_1 –, θ_2 – or d_3 – motors reaches a mechanical limit (actually a software limit acts before the motor has reached a mechanical limit), we are losing our redundant DOF, but can still follow a desired path (until a second motor reaches a mechanical limit). To solve this, $\underline{\dot{\theta}}$ is first calculated by means of Equation [**26**]. If the θ_1 – motor is at a mechanical limit and Equation [**26**] shows that the motor should pass through the mechanical limit, we have to perform a second calculation exactly as described in the section Velocity limitations, but now with $\dot{\theta}_{1\,max}$ replaced by 0. Similar calculations are made for θ_2 and d_3 when they reach their mechanical limits.

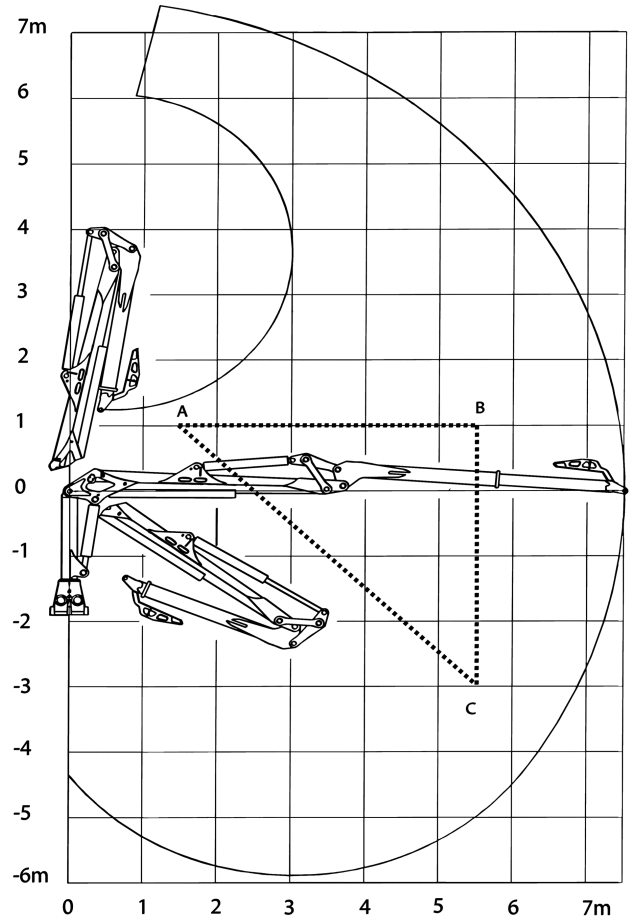

Figure 8. ~ *Workspace and simulation task.*

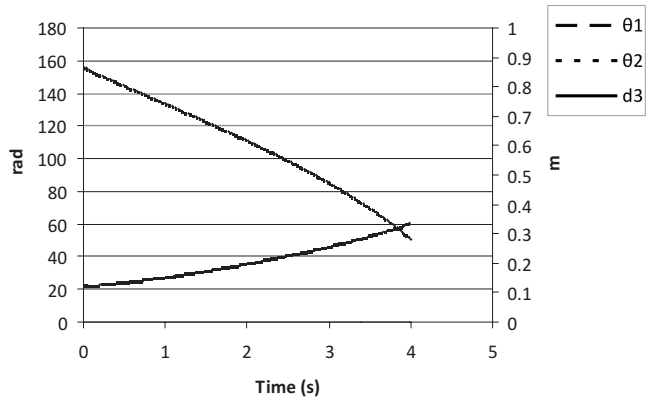

Figure 9. ~ *TCP moves from A to B with a speed of 1.0 m/s. Variations in* θ_1 *and* θ_2. d_3 *is not moving.*

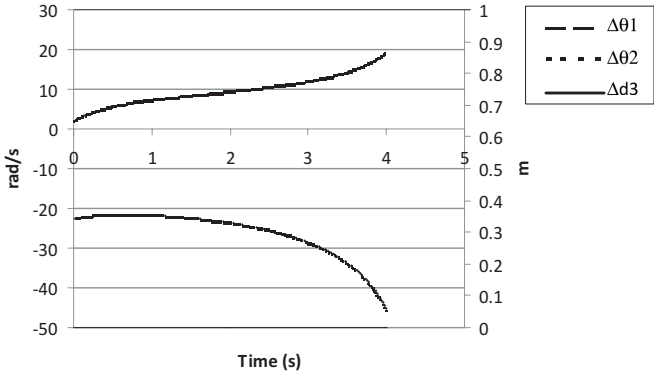

Figure 10. ~ *TCP moves from A to B with a speed of 1.0 m/s. Variations in* $\dot{\theta}_1, \dot{\theta}_2$, *and* d_3 *is not moving.*

In order to avoid large transients when approaching a mechanical limit, the maximum velocity used for calculations is decreased for that motor.

Simulations

The maximum lifting capacity control algorithm has been tested through simulations in a program developed especially for this work. The simulations are conducted for a common manipulator driven by hydraulic actuators. We have limited the simulations to one typical task. The task describes a normal working cycle, which occurs when a forwarder is loading and unloading logs from the ground and off/on the carrier. The task consists of three linear segments (ABC) in the workspace as shown in **Figure 8**. The paths are as follows: A – B, B – C, and C – A. For each path, the position and velocity of the joints are analyzed. The coordinates for each point in the work space are:

A (1.5, 1.0)

B (5.5, 1.0)

C (5.5, –3.0)

For the simulations, we have used the following data. Workspace of the boom Cranab 850 is seen in **Figure 8**. The joint limits are:

$$\theta_{1\,\min} = 8\text{deg}$$
$$\theta_{1\,\max} = 123\text{deg}$$
$$\theta_{2\,\min} = 2\text{deg}$$
$$\theta_{2\,\max} = 178\text{deg}$$
$$d_{3\,\min} = 0m$$
$$d_{3\,\max} = 1.4m$$
$$r_c = 3.5m$$
$$z_c = 0.65m$$
$$\rho_{\min} = 3.5m$$
$$\rho_{\max} = 4.9m$$

The maximum velocities of the joints that are used for all of the simulations are:

$$\dot{\theta}_{1\,\max} = 0.88\ rad/s$$
$$\dot{\theta}_{2\,\max} = 1.23\ rad/s$$
$$\dot{d}_{3\,\max} = 0.42\ m/s$$

The joint speeds are set to be equal in both directions. This is due to the fact that for each machine application the hydraulic pressure and flow are different. Therefore, the joint speeds are set corresponding to one typical pressure and flow.

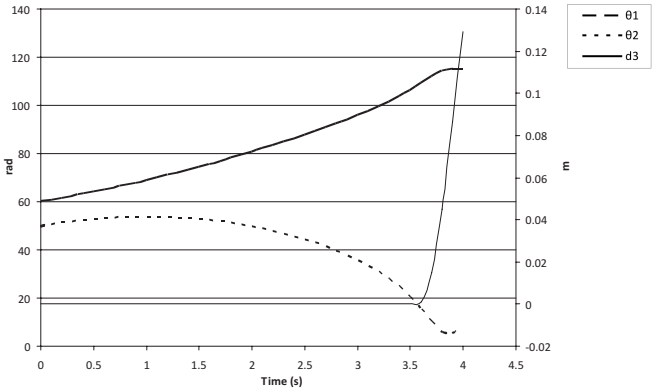

Figure 11. ~ *TCP moves from B to C with a speed of 1.0 m/s. Variations* θ_1, θ_2, *and* d_3.

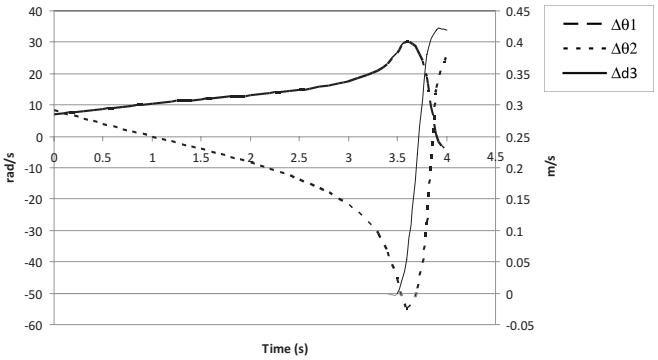

Figure 12. ~ *TCP moves from B to C with a speed of 1.0 m/s. Variations in* $\dot{\theta}_1$, $\dot{\theta}_2$, *and* d_3.

The following figures from the simulations show the time records of θ_1, θ_2, d_3, $\dot{\theta}_1$, $\dot{\theta}_2$, and $\dot{d}_3$ when the TCP moves from point A to B, B to C, and C to A in the workspace at the velocity of 1.0 m/s. The theoretically achievable positioning times at these speeds are as follows:

A to B and B to C: 4 s

C to A: 5.66 s

If these times are not met, it is an indication that one or more of the DOFs are saturated.

The joints are limited to maximum allowed velocities. To be able to display d_3 on the same plot as θ_1 and θ_2, d_3 has been multiplied with a constant set to 100.

TCP moves from point A to B (**Figs. 9 and 10**). The algorithm needs 4.0 s to go from point A to B, which is the same time as the theoretical achievable time. The velocities of the joints change smoothly in both cases. Only the joints $\dot{\theta}_1$ and $\dot{\theta}_2$ are used and none of the joint velocities reach their speed limits.

TCP moves from point B to C (**Figs. 11 and 12**). The algorithm needs 4.0 s to go from point B to C. d_3 reaches its maximum velocity limit.

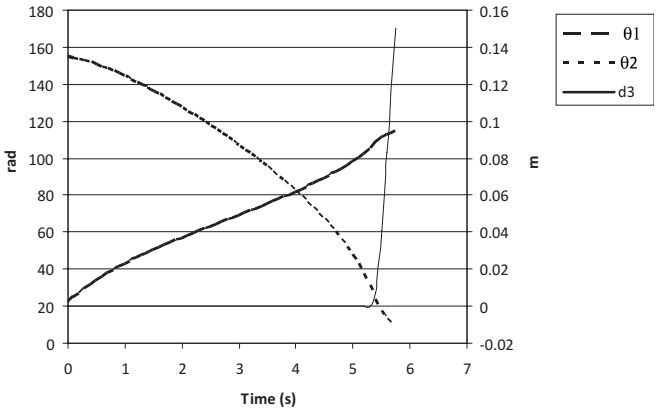

Figure 13. ~ *TCP moves from C to A with a speed of 1.0 m/s. Variations* θ_1, θ_2, *and* d_3.

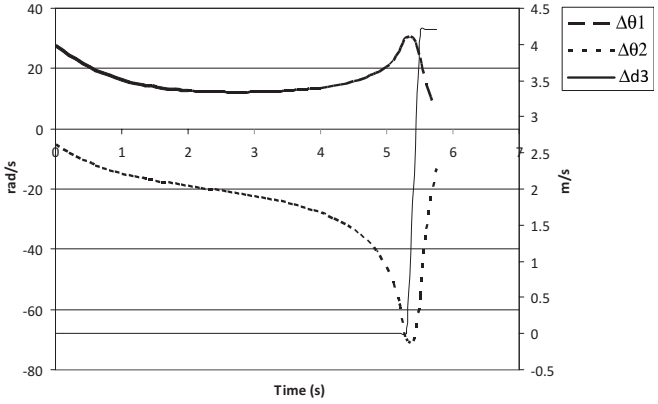

Figure 14. ~ *TCP moves from C to A with a speed of 1.0 m/s. Variations in* $\dot{\theta}_1$, $\dot{\theta}_2$, *and* d_3.

TCP moves from point A to C (**Figs. 13 and 14**). The algorithm needs 5.77 s to go from point A to C, which is 0.11 s longer than the theoretically achievable time. θ_2 and d_3 reach their maximum velocity limits. A scaling of the commanded signal is necessary, which increases the time consumption. During scaling, the path is followed, but with a lower velocity than 1.0 m/s.

Conclusions

An algorithm for computation of the inverse kinematics of kinematically redundant hydraulic manipulators was investigated. The hydraulic manipulator used in the simulation study consists of a 4-DOF hydraulic forestry machine manipulator. The simulations show the necessary speed requirements for all of the joints when performing straight paths in the manipulator work area. The simulations also show time consumption and also what happens when the joints reach their maximum velocity limit.

Although this work was an attempt to propose complete algorithms that could be directly applicable to a real system, it is still only a simulation study which lacks the qualities of implementation on a real hydraulic manipulator.

In future work the maximum lifting capacity method will be tested in a forestry real-time simulator. The method will be evaluated by forestry machine operators to determine if boom tip control could increase productivity. Semi-automated functions will also be tested.

Acknowledgment

The authors wish to express their sincere gratitude to all of those who have supported them and made this work possible. In particular they would like to mention Charles Davidson, PhD, for skillful and stimulating supervision and especially for good advice on the theoretical section of this paper.

Literature Cited

Ahlgren, T., L. Brundin, B. Jonsson, C. Löfroth, B. Morenius, and D. Myhrman. 1982. Maneuver system for hydraulic cranes. Skogforsk Redogörelse nr 6. In Swedish.

Beiner, L. and J. Mattila. 1999. An improved pseudo-inverse solution for redundant hydraulic manipulators. Robotica, 17: 173-179.

Chan, T.F. and R.V. Dubey. 1995. A weighted least-norm solution based scheme for avoiding joint limits for redundant joint manipulators. IEEE Trans. on Robotics and Automation. 11(2): 286-292.

Chen, W., Q. Zhang, Z. Yang, and W.A. Gruver. 1995. Optimizing multiple performance criteria in redundant manipulators by subtask-priority control. *In*: Proc. of the 1995 IEEE International Conf. on Systems, Man, and Cybernetics, Vancouver, Canada, Oct. pp. 2534-2539.

Chen, W., Q. Zhang, Z. Yang, and W.A. Gruver. 1995. A new approach to the kinematic control of redundant manipulators. *In*: Proc. of the 1995 IEEE International Conf. on Systems, Man, and Cybernetics, Vancouver, Canada, Oct. pp. 2528-2533.

Cleary, K. and C. Tesar. 1990. Incorporating multiple criteria in the operation of redundant manipulators. IEEE Int. Conf. Robotics and Automation, Cincinnati. pp. 618-623.

Erikson, G. and M. Thor. 1999. Interaction human-forest machine. Report from a SLO-project. Skogforsk Arbetsrapport 423. In Swedish.

Gellerstedt, S. 1993. Thinning with a forestry machine – the mental and physical stress. Uppsatser och resultat nr. 244. Inst. F. Forest Technology. The Agricultural University of Sweden. In Swedish.

Hollerbach, J.M. and K.C. Suh. 1986. Redundancy resolution of manipulators through torque optimization. A. I. Memo 882, Massachusetts Institute of Technology, Jan.

Honegger, M. and A. Codourey. 1998. Redundancy resolution of a Cartesian space operated heavy industrial manipulator. Int. Conf. on Robotics and Automation, May 16-21.

Honzik, B. and F. Zezulka. 1999. Redundancy resolution techniques for mobile manipulators. AMPTS '99.

Klein, C.A. 1985. Use of redundancy in the design of robotic systems. *In*: Robotic Research: The Second Int. Symposium, H. Hanafusa and H. Inoue, Eds. MIT Press, Cambridge, MA. pp. 208-214.

Klein, Charles A. and Koh-Boon Kee. 1989. The nature of drift in pseudo inverse control of kinematically redundant manipulators. IEEE Transactions on Robotics and Automation. 5(2): 231-234.

Li, L., W.A. Gruver, and Q. Zhang. 2001. Kinematic control of redundant robots based on the motion optimizability measure, IEEE Transactions on Systems, Man and Cybernetics, 2001, Part B, vol. 31, no. 1.

Löfgren, B. 1989. Boom tip control. Skogforsk. Meddelande No. 18, Forest Research Institute of Sweden. In Swedish.

Löfgren, B., M. Landström, M. Atterbrandt, N. Pettersson, and B. Nordén. 1994. Boom tip control – an evaluation. Skogforsk. Redogörelse, Nr.1, 1994. In Swedish.

Martin, D.P., J. Baillieul, and J.M. Hollerbach. 1989. Resolution of kinematic redundancy using optimization techniques. IEEE Transaction on Robotics and Automation. 5(4): 529-533.

McGee, S., T.F. Chan, and R.V. Dubey. 1994. Probability weighting of performance criteria for a redundant manipulator. IEEE. pp. 1887-1894.

Nakamura, Y. 1991. Advanced Robotics, Redundancy and Optimization. Addison-Wesley.

Nedungadi, A. 1987. Torque optimization of redundant manipulators. Int. Symp. on Intelligent Robotics. pp. 10.65-10.83.

Nedungadi, A. and K. Kazerounian. 1989. A local solution with global characteristics for the joint torque optimization of a redundant manipulator. J. of Rob. Systems. 6(5): 631-654.

Nenchev, D. N. 1987. Redundancy resolution through local optimization: A review. J. of Rob. Systems. 6(6): 769-798.

Noble, B. 1975. Methods for computing the Moore-Penrose Generalized Inverse, and related matters. M.Z. Nashed Ed. Academic Press, NY. pp. 254-301.

Sciavicco, L. and B. Siciliano. 1987. A Dynamic Solution to the Inverse Kinematic Problem for Redundant Manipulators. *In*: Proc. IEEE Int. Conf. Robotics and Automation. pp. 1081-1087.

Siciliano, B. 1990. Kinematic control of redundant manipulators: A tutorial. J. of Int. and Rob. Systems. 3: 201-212.

SkogForsk. 1994. A number of productivity and time studies under the period 1970-2002. Brunberg, T. Westerlund, M. Studie av Timberjack 1270, Timberjack 1880 och Valmet 911 vid Djupdal, SCA Skog AB.

Suh, K.C. and J.M. Hollerbach. 1987. Local versus global torque optimization of redundant manipulators. IEEE Int. Conf. Robotics and Automation. pp. 619-624.